Formation of Bridging Acylium and Nitrilium Complexes by Reaction of CO and $CNC(CH_3)_3$ with a Bridging Diiron Methylidyne Complex. Evidence for Strong Electron Donation from the Fe_2C Core onto the μ-CHC≡O and μ-CHC≡NR Ligands

Charles P. Casey,* Mark Crocker, Gerald P. Niccolai, Paul J. Fagan, and Mark S. Konings

Contribution from the Department of Chemistry, University of Wisconsin, Madison, Wisconsin 53706. *Received October 2, 1987*

Abstract: The reaction of the μ-methylidyne complex $[C_5H_5(CO)Fe]_2(\mu\text{-}CO)(\mu\text{-}CH)^+PF_6^-$ (**1**) with CO gave the cationic 1:1 adduct $[C_5H_5(CO)Fe]_2(\mu\text{-}CO)(\mu\text{-}CHCO)^+PF_6^-$ (**2**) in 90% yield. The structure, spectra, and chemical properties of **2** suggest that the bonding of the μ-CHCO ligand in **2** should be regarded as analogous to that in organic acylium cations, with a contributing formulation as a two-electron three-center bound-bridging ketene. **2** reacted with nucleophiles at the acylium carbon; reaction with $Et_4N^+HFe(CO)_4^-$ gave the aldehyde $[C_5H_5(CO)Fe]_2(\mu\text{-}CO)(\mu\text{-}CHCHO)$ (**3**), water gave the carboxylic acid $[C_5H_5(CO)Fe]_2(\mu\text{-}CO)(\mu\text{-}CHCO_2H)$ (**4**), and ammonia gave the amide $[C_5H_5(CO)Fe]_2(\mu\text{-}CO)(\mu\text{-}CHCONH_2)$ (**5**). **1** also reacted with $CNC(CH_3)_3$ to give the 1:1 adduct $[C_5H_5(CO)Fe]_2(\mu\text{-}CO)[\mu\text{-}CHCNC(CH_3)_3]^+PF_6^-$ (**6**), the structure of which was determined by X-ray crystallography: **6** crystallizes in the monoclinic space group $P2_1/c$, with unit cell constants a = 10.771 (2) Å, b = 11.420 (2) Å, c = 18.092 (3) Å, β = 106.09 (1)°, and Z = 4. The μ-ethylidyne complex $[C_5H_5(CO)Fe]_2(\mu\text{-}CO)(\mu\text{-}CCH_3)^+BF_4^-$ (**7**) underwent a similar reaction with $CNC(CH_3)_3$ to afford the adduct $[C_5H_5(CO)Fe]_2(\mu\text{-}CO)[\mu\text{-}C(CH_3)CNC(CH_3)_3]^+BF_4^-$ (**8**), which was isolated as a mixture of two cis and one trans Cp isomers. The structure of **6**, together with the spectroscopic properties of **6** and **8**, suggests an analogous bonding mode to that in **2**. Fenske-Hall molecular orbital calculations performed on **2** and **6** provide further support for the importance of a ketene-like formulation that contributes to the overall structure of these complexes.

The diiron methylidyne complex $[C_5H_5(CO)Fe]_2(\mu\text{-}CO)(\mu\text{-}CH)^+PF_6^-$ (**1**) forms 1:1 adducts with a variety of heteroatom and carbon nucleophiles such as NMe_3.[1] **1** is also sufficiently electrophilic to react with alkenes via addition of the methylidyne C-H bond across the carbon-carbon double bond of the alkene, which produces new μ-alkylidyne complexes in a hydrocarbation reaction.[2,3]

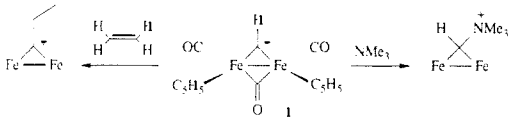

Since the interaction of carbon monoxide with small carbon fragments bound to metal atoms is thought to be important in CO reduction and related chemistry,[4,5] we have studied the reaction of **1** with CO. Here we report full details in the reaction of **1** with CO that produces a 1:1 adduct $[C_5H_5(CO)Fe]_2(\mu\text{-}CO)(\mu\text{-}CHCO)^+PF_6^-$ (**2**).[6] To adequately explain the structure, spectra, and chemical properties of this adduct, two resonance structures must be considered. The major resonance contributor is the acylium formulation **2a**, which is similar to acylium cations such as $CH_3C{\equiv}O^+$. The minor resonance contributor is the ketene formulation **2k** in which the CH=C=O group interacts with the diiron center by a three-center two-electron bond; this formulation helps to explain the short carbon-carbon bond of the μ-CHCO ligand and delocalization of positive charge onto the iron framework.

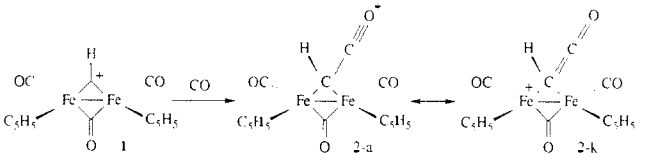

Fenske-Hall molecular orbital calculations that support the importance of these two formulations will be presented. In addition, the structure and spectra of a 1:1 adduct of **1** with *tert*-butyl isocyanide provide further experimental support for the importance of resonance structures analogous to ketene formulation **2k**.

Results

Reaction of CO with 1. When a slurry of **1** in CH_2Cl_2 was stirred under a CO atmosphere (600 Torr) for 2 h at room temperature, a color change from deep red to purple-black was observed. Addition of diethyl ether and filtration afforded the CO adduct $[C_5H_5(CO)Fe]_2(\mu\text{-}CO)(\mu\text{-}CHCO)^+PF_6^-$ (**2**) as a purple-black crystalline solid in 90% yield. Similarly, reaction of **1** with 90% enriched ^{13}CO gave the corresponding μ-$CH^{13}CO$ complex **2**-^{13}**C**.

In the ^1H NMR spectrum of **2**, a singlet at δ 6.94 is assigned to the μ-CHCO ligand and a singlet at δ 5.67 is assigned to the equivalent cis C_5H_5 groups. The ^{13}C NMR spectrum contains a singlet C_5H_5 resonance (δ 90.6, $J_{^{13}C-H}$ = 183 Hz), together with a single terminal CO resonance at δ 209.2 and a resonance for the bridging carbonyl ligand at δ 249.6. The carbons of the μ-CHCO unit appear at δ 162.6 (μ-*C*HCO) and 27.5 (μ-C*H*CO, $J_{^{13}C-H}$ = 174 Hz). In the ^1H NMR spectrum of **2**-^{13}**C**, the res-

(1) Casey, C. P.; Crocker, M.; Vosejpka, P. C.; Fagan, P. J.; Marder, S. R.; Gohdes, M. A. *Organometallics* **1988**, *7*, 670-675.
(2) Casey, C. P.; Meszaros, M. W.; Fagan, P. J.; Bly, R. K.; Marder, S. R.; Austin, E. A. *J. Am. Chem. Soc.* **1986**, *108*, 4043-4053.
(3) Casey, C. P.; Meszaros, M. W.; Fagan, P. J.; Bly, R. K.; Colborn, R. E. *J. Am. Chem. Soc.* **1986**, *108*, 4053-4059.
(4) (a) Herrmann, W. A. *Angew. Chem., Int. Ed. Engl.* **1982**, *21*, 117-130. (b) Shriver, D. F. *ACS Symp. Ser.* **1981**, *152*, 1-18. (c) Muetterties, E. L.; Stein, J. *Chem. Rev.* **1979**, *79*, 479-490. (d) Ponec, V. *Catal. Rev.-Sci. Eng.* **1978**, *18*, 151-171. (e) Biloen, P.; Helle, J. N.; Sachtler, W. M. H. *J. Catal.* **1979**, *58*, 95-107. (f) Masters, C. *Adv. Organomet. Chem.* **1979**, *17*, 61-103.
(5) For the interaction of carbon monoxide with mononuclear metal carbynes, see, for example: (a) Sheridan, J. B.; Geoffroy, G. L.; Rheingold, A. L. *Organometallics* **1986**, *5*, 1514-1515. (b) Churchill, M. R.; Wasserman, H. J.; Holmes, S. J.; Schrock, R. R. *Organometallics* **1982**, *1*, 766-768. (c) Kreissl, F. R.; Frank, A.; Schubert, U.; Lindner, T. L.; Huttner, G. *Angew. Chem., Int. Ed. Engl.* **1976**, *15*, 632-633. (d) Uedelhoven, W.; Eberl, K.; Kreissl, F. R. *Chem. Ber.* **1979**, *112*, 3376-3389 and references therein.
(6) Casey, C. P.; Fagan, P. J.; Day, V. W. *J. Am. Chem. Soc.* **1982**, *104*, 7360-7361.

0002-7863/88/1510-6070$01.50/0

Table I. Selected Bond Distances and Angles for $[C_5H_5(CO)Fe]_2(\mu\text{-}CO)(\mu\text{-}CH)^+PF_6^-$ (**2**)

	(a) Bond Distances (Å)		
Fe–Fe′	2.548 (1)	C_1–O_1	1.135 (7)
Fe–C_t	1.776 (4)	C_t–O_t	1.134 (7)
Fe–C_b	1.948 (4)	C_b–O_b	1.164 (7)
Fe–C	1.994 (4)	C–C_1	1.338 (8)
Fe–C_g[a]	1.730 (–)		
	(b) Bond Angles (deg)		
C–C_1–O_1	174.9 (6)	Fe–C–Fe′	79.4 (2)
H–C–C_1	111 (2)	C_b–Fe–C	99.2 (2)
Fe–C–C_1	110.6 (3)	C_t–Fe–C_b	89.2 (2)
Fe–C–H	121 (2)	C_t–Fe–C	97.9 (2)
Fe–C_t–O_t	177.7 (4)	Fe′–Fe–Cg	137.6 (–)
Fe–C_b–O_b	139.1 (1)	Cg–Fe–Ct	122.1 (–)
Fe–C_b–Fe′	81.7 (2)	Cg–Fe–C_b	118.3 (–)
Cg–Fe–C	123.0 (–)		

[a] C_g = center of gravity of Cp group.

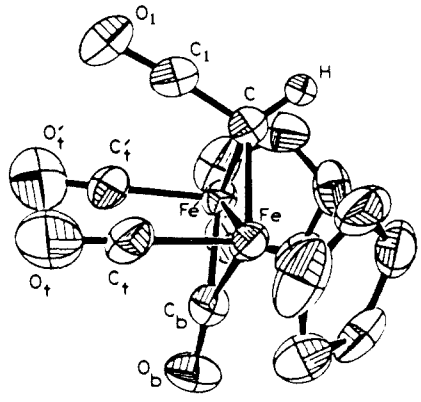

Figure 1. ORTEP drawing of the cation of **2**.

onance due to the μ-CH^{13}CO ligand at δ 6.94 appears as a doublet with $^2J_{^{13}C-H}$ = 4.4 Hz. No evidence for scrambling of the ^{13}C label with the metal-bound carbonyl ligands of **2**-^{13}**C** was detected by IR or NMR spectroscopy. The infrared band for the μ-CHCO carbonyl of **2** appears at 2092 cm^{-1} and is shifted to 2057 cm^{-1} for **2**-^{13}**CO**, while the bands for the terminal and bridging CO ligands at 2002 and 1819 cm^{-1} remain unchanged.

The molecular structure of **2** was determined by X-ray crystallography[6] and consists of discrete $[C_5H_5(CO)Fe]_2(\mu\text{-}CO)(\mu\text{-}CHCO)^+$ cations and PF_6^- anions (Figure 1). The cation possesses rigorous crystallographic C_s-*m* symmetry with the μ-CHCO and μ-CO ligands lying in the mirror plane at x = 0 in the lattice. The carbonyl group of the μ-CHCO ligand is directed in an anti orientation relative to the cis C_5H_5 ligands of **2**. Formation of this stereoisomer is the result of nucleophilic attack of CO on the μ-CH ligand of **1** from the side opposite to the relatively large C_5H_5 rings. The μ-CHCO unit is nearly linear and has a C–C–O angle of 174.9 (6)°.

A comparison of the bond lengths of the μ-CHCO ligand of **2** with those of the acylium cation $CH_3C{\equiv}O^+SbF_6^-$[7] reveals that the C–C bond of the μ-CHCO ligand (1.338 (8) Å) is 0.047 Å shorter than that of $CH_3C{\equiv}O^+$ (1.385 (16) Å) and that the C–O bond of the μ-CHCO ligand (1.135 (7) Å) is 0.027 Å longer than that of $CH_3C{\equiv}O^+$. This suggests that in addition to the acylium formulation **2a** for the μ-CHCO ligand, there is also some ketene-like character in the ligand which may be explained in terms of a contribution to the overall structure from the ketene formulation **2k**. Further support for contribution from the ketene formulation **2k** is provided by the carbonyl stretch of the μ-CHCO ligand in **2** which is observed at 2092 cm^{-1}. This stretch occurs at substantially lower energy than that of $CH_3C{\equiv}O^+SbF_6^-$ (2300 cm^{-1})[7] and falls in the range generally observed for organic ketenes (2000–2200 cm^{-1}).[8]

Reactions of Nucleophiles with 2. The bridging acylium complex **2** was readily attacked by nucleophiles at the acylium carbonyl carbon. This behavior is typical of organic acylium cations. When a slurry of **2** and $Et_4N^+HFe(CO)_4^-$ was stirred in THF, a deep red solution formed from which the aldehyde-substituted μ-alkylidene complex $[C_5H_5(CO)Fe]_2(\mu\text{-}CO)(\mu\text{-}CHCHO)$ (**3**) was isolated in 70% yield. **3** was also synthesized in 50% yield by the addition of $K^+HB[OCH(CH_3)_2]_3^-$ to a THF slurry of **2**.

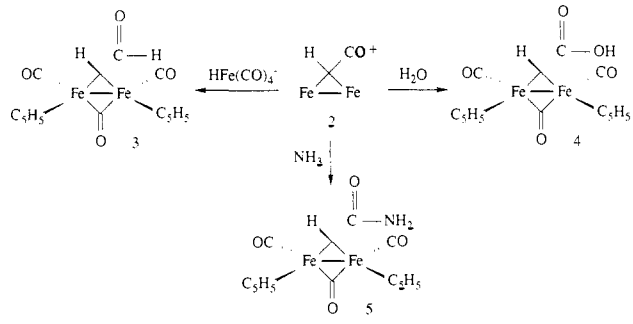

The structure of **3** was readily established spectroscopically. The presence of a μ-CHCHO ligand is supported by the observation of two doublets with characteristic downfield chemical shifts of δ 10.26 and 9.63, each showing the same 9.3-Hz coupling. In the $^{13}C\{^1H\}$ NMR spectrum, signals are observed for the bridging alkylidene carbon at δ 156.1 and for the aldehyde carbon at δ 202.2. The infrared spectrum of **3** contains bands due to the terminal and bridging carbonyl ligands at 1990 (s), 1956 (m), and 1800 (s) cm^{-1}, as well as a band at 1615 cm^{-1} assigned to the carbonyl of the aldehyde group.

Water also adds readily to the acylium carbon of complex **2**. Addition of H_2O to a slurry of **2** in CH_2Cl_2 afforded a red precipitate of the carboxylic acid $[C_5H_5(CO)Fe]_2(\mu\text{-}CO)(\mu\text{-}CHCO_2H)$ (**4**), which was isolated in 40% yield. The ^1H NMR spectrum of **4** contains a downfield singlet at δ 10.34 assigned to the μ-alkylidene proton of the μ-$CHCO_2H$ ligand and a broad resonance at δ 9.85 assigned to the carboxylic acid proton. In the ^{13}C NMR spectrum, the bridging carbon appears as a doublet at δ 142.3 ($J_{^{13}C-H}$ = 139 Hz) and the CO_2H carbon appears as a singlet at δ 184.3. The IR spectrum of **4** also supports its formulation as a carboxylic acid, containing a broad band at 2930 cm^{-1} characteristic of O–H stretching, a band at 1630 cm^{-1} corresponding to C=O stretching, as well as bands at 1440 and 1284 cm^{-1} due to O–H bending and C–O stretching.[9]

The reaction of **2** with anhydrous ammonia in CH_2Cl_2 produced a red solution from which the amide $[C_5H_5(CO)Fe]_2(\mu\text{-}CO)(\mu\text{-}CHCONH_2)$ (**5**) was isolated in 28% yield. The formulation of **5** as an amide was based on spectroscopic characterization. In the ^1H NMR spectrum of **5**, two broad singlets integrating for one proton each are observed at δ 7.25 and 6.29, characteristic of protons bound to nitrogen. In the ^{13}C NMR spectrum, a resonance at δ 183.4 is attributed to the amide carbon. The IR spectrum of **5** contains bands at 3515 and 3384 cm^{-1} characteristic of asymmetric and symmetric N–H stretching vibrations, respectively, while bands at 1629, 1579, and 1338 cm^{-1} are attributed to N–H bending (amide II band), C=O stretching (amide I band), and C–N stretching, respectively.[9]

Reaction of 1 with CNCMe$_3$. The reaction of **1** with *tert*-butyl isocyanide was examined to test structural predictions implicit in the μ-ketene formulation **2k**. Two resonance formulations are possible for the isocyanide adducts: the nitrilium formulation **6n** and the ketenimine formulation **6k**. If the ketenimine resonance structure is an important contributor, then the μ-CHCNCMe$_3$

(7) (a) Boer, F. P. *J. Am. Chem. Soc.* **1968**, *90*, 6706–6710. (b) See also: Olah, G. A.; Germain, A.; White, A. M. *Carbonium Ions*; Wiley-Interscience: New York, 1976; Vol. 5, pp 2102–2107 and reference therein.

(8) See, for example: Dolphin, D.; Wick, A. E. *Tabulation of Infrared Spectral Data*; Wiley-Interscience: New York, 1977; Chapter 4, pp 408–409 and references therein.

(9) Silverstein, R. M.; Bassler, G. C.; Morrill, T. C. *Spectrometric Identification of Organic Compounds*; John Wiley and Sons: New York, 1981; Chapter 3.

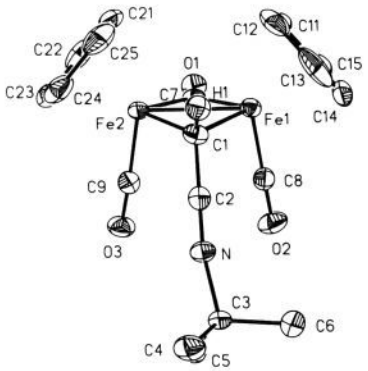

Figure 2. ORTEP drawing of the cation of **6**.

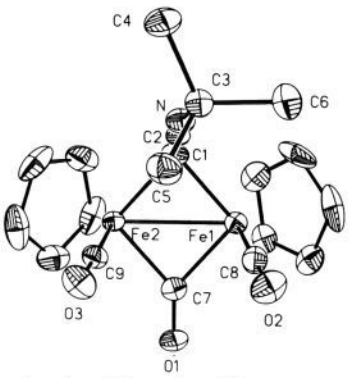

Figure 3. ORTEP drawing of the cation of **6**.

ligand should be *bent* at nitrogen and the *tert*-butyl group should be laterally displaced along a line parallel to the iron–iron bond.

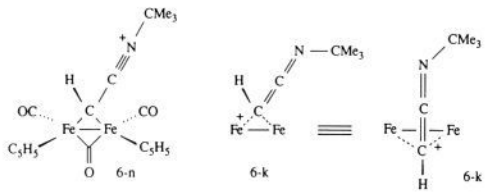

Addition of $CNCMe_3$ to a dichloromethane slurry of **1** at −78 °C followed by warming to room temperature resulted in a color change from deep red to purple. Evaporation of volatile material under high vacuum and recrystallization of the residue from CH_2Cl_2/diethyl ether led to the isolation of the isonitrile adduct $[C_5H_5(CO)Fe]_2(\mu\text{-}CO)[\mu\text{-}CHCNC(CH_3)_3]^+PF_6^-$ (**6**) as a purple-red solid in 63% yield.

The ^1H NMR spectrum of **6** establishes that **6** is a 1:1 adduct of **1** and $CNCMe_3$. Singlets are observed at δ 1.51 for the *tert*-butyl group, at δ 5.14 for the two cis C_5H_5 groups, and at δ 7.73 for the proton attached to the bridging carbon atom. In the $^{13}C\{^1H\}$ NMR spectrum of **6**, the resonance due to the bridging alkylidene carbon of the μ-$CHCNCMe_3$ ligand appears δ 61.6, and the μ-$CHCNCMe_3$ carbon appears as a very broad resonance at δ 125.7. The IR spectrum shows a resonance at 2232 cm^{-1} corresponding to C≡N stretching in addition to bands for the carbonyl ligands.

In order to gain further insight into the structure and bonding of **6**, a single-crystal X-ray diffraction study was undertaken. The molecular structure of **6** consists of discrete $[C_5H_5(CO)Fe]_2(\mu\text{-}CO)[\mu\text{-}CHCNC(CH_3)_3]^+$ cations (Figures 2 and 3) and PF_6^- anions. The μ-$CHCNCMe_3$ ligand is best described as a nitrilium species, having a C(2)–N multiple bond length of 1.147 (4) Å and a nitrilium carbon to μ-alkylidene carbon (C2–C1) bond length of 1.397 (5) Å. As in the case of acylium complex **2**, the nitrilium complex **6** is formed by attack of $CNCMe_3$ from the side opposite the C_5H_5 ligands of **1**. However, unlike the acylium complex **2**, the cation of **6** does not possess mirror symmetry due to the nonlinearity of the μ-$CHCNCMe_3$ ligand. The C1–C2–N angle is nearly linear at 177.9 (4)° and these three atoms lie in a plane perpendicular to and bisecting the Fe–Fe vector. The C2–N–C3 angle is bent at 169.5 (4)° such that the *tert*-butyl group is displaced along a line parallel to the Fe–Fe axis. While the magnitude of the distortion from linearity is only moderate, the direction of this distortion is precisely that expected if the ketenimine formulation **6k** is a significant resonance contributor.

Table II. Selected Bond Distances and Angles for $[C_5H_5(CO)Fe]_2(\mu\text{-}CO)[\mu\text{-}CHCNC(CH_3)_3]^+PF_6^-$ (**6**)

	(a) Bond Distances (Å)		
Fe(1)–Fe(2)	2.534 (1)	Fe(1)–C(1)	1.977 (4)
Fe(1)–C(7)	1.937 (4)	Fe(1)–C(8)	1.769 (3)
Fe(2)–C(7)	1.933 (4)	Fe(2)–C(1)	1.978 (4)
C(1)–C(2)	1.397 (5)	Fe(2)–C(9)	1.766 (3)
N–C(3)	1.468 (5)	C(2)–N	1.147 (4)
C(1)–H(1)	1.01 (4)		
	(b) Bond Angles (deg)		
Fe(2)–Fe(1)–C(1)	50.2 (1)	Fe(2)–Fe(1)–C(7)	49.0 (1)
C(1)–Fe(1)–C(7)	98.8 (2)	Fe(2)–Fe(1)–C(8)	99.3 (1)
C(1)–Fe(1)–C(8)	95.7 (2)	C(7)–Fe(1)–C(8)	89.4 (2)
C(1)–Fe(2)–C(7)	98.9 (2)	Fe(1)–Fe(2)–C(7)	49.2 (1)
C(1)–Fe(2)–C(9)	95.2 (1)	Fe(1)–Fe(2)–C(9)	99.5 (1)
Fe(1)–C(1)–Fe(2)	79.7 (1)	C(7)–Fe(2)–C(9)	90.0 (2)
Fe(2)–C(1)–H(1)	119.2 (20)	Fe(1)–C(1)–H(1)	114.1 (23)
Fe(1)–C(1)–C(2)	116.1 (3)	C(2)–C(1)–H(1)	107.3 (20)
C(1)–C(2)–N	177.9 (4)	Fe(2)–C(1)–C(2)	118.5 (3)
Fe(1)–C(7)–Fe(2)	81.8 (1)	C(2)–N–C(3)	169.5 (4)
Fe(2)–C(7)–O(1)	139.6 (3)	Fe(1)–C(7)–O(1)	138.5 (3)
Fe(2)–C(9)–O(3)	177.6 (4)	Fe(1)–C(8)–O(2)	179.2 (4)

Reaction of the Ethylidyne Complex $[C_5H_5(CO)Fe]_2(\mu\text{-}CO)(\mu\text{-}CCH_3)^+BF_4^-$ with $CNCMe_3$. While the methylidyne complex **1** is sufficiently electrophilic to form 1:1 adducts with CO and $CNCMe_3$, other cationic diiron μ-alkylidyne complexes such as the ethylidyne species $[C_5H_5(CO)Fe]_2(\mu\text{-}CO)(\mu\text{-}CCH_3)^+BF_4^-$ (**7**) were found to be inert to CO under similar reaction conditions. However, when $CNCMe_3$ was added to a slurry of ethylidyne complex **7** in CH_2Cl_2, a color change from red to purple-red was observed and the $CNCMe_3$ adduct $[C_5H_5(CO)Fe]_2(\mu\text{-}CO)[\mu\text{-}C(CH_3)CNC(CH_3)_3]^+BF_4^-$ (**8**) was isolated in 89% yield.

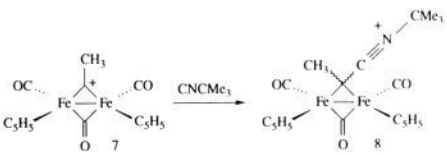

The spectral characteristics of **8** are similar to those of **6**. However, one major difference lies in the observation that **8** exists as a mixture of two cis and one trans Cp isomers, as indicated by the ^1H and $^{13}C\{^1H\}$ NMR spectra. In the ^1H NMR spectrum of **8** three sets of singlets are observed for both the *t*-Bu protons and the methyl protons of the μ-$C(CH_3)CNC(CH_3)_3$ group. In the cyclopentadienyl region of the spectrum, two resonances are observed corresponding to two cis Cp isomers, together with a pair of resonances of lesser intensity corresponding to the inequivalent Cp groups of the trans isomer. These two cis isomers differ in the relationship between the Cp ligands and the $CNCMe_3$ group on the bridging alkylidene carbon. Integration of the ^1H NMR spectrum indicates a 4.1:1.2:1.0 ratio for the cis:cis′:trans isomers. In the ^{13}C NMR spectrum, this pattern was repeated for the carbons of the Cp, CH_3, and *t*-Bu groups. Since the starting methylidyne complex **1** exists predominantly as the cis isomer (>95% by ^1H NMR), the isomers observed for **8** presumably represent a thermodynamic mixture deriving from the similar steric properties possessed by the CH_3 and $CNCMe_3$ substituents on the bridging alkylidene carbon. Such cis–trans isomerizations have been well documented for diiron complexes.[10,11]

(10) Casey, C. P.; Fagan, P. J.; Miles, W. H. *J. Am. Chem. Soc.* **1982**, *104*, 1134–1136.
(11) Dyke, A. F.; Knox, S. A. R.; Morris, M. J.; Naish, P. J. *J. Chem. Soc., Dalton Trans.* **1983**, 1417–1426.

Finally, the irreversibility of formation of **8** was demonstrated. When equimolar amounts of **8** and methylidyne complex **1** were mixed in CD_2Cl_2 and the solution monitored by ^1H NMR spectroscopy, the only changes observed in the ^1H NMR spectrum resulted from the gradual thermal decomposition of **1**. No evidence for transfer of *tert*-butyl isocyanide from **8** to the more electrophilic **1** was observed.

Discussion

The experimental evidence presented here indicates that the bonding of the μ-CHCO ligand in **2** requires the consideration of two resonance contributors. The major resonance contributor **2a** is analogous to that of acylium cations such as $CH_3C{\equiv}O^+$. The minor resonance contributor **2k** has a two-electron three-center bound-bridging ketene. While **2** exhibits chemical reactivity similar to organic acylium cations, structural and infrared data are indicative of some ketene character in the μ-CHCO ligand. More specifically, in the crystal structure of **2** the C–C distance of 1.338 (8) Å in the μ-CHCO unit is 0.05 Å shorter than that in the cation $CH_3C{\equiv}O^+SbF_6^-$,[7] while it is 0.03 Å longer than the C–C bond of $CH_2{=}C{=}O$ (1.31 (1) Å)[12] and $(CH_3)HC{=}C{=}O$ (1.306 (2) Å).[13] Similarly, the C–O bond length of 1.135 (7) Å for the μ-CHCO ligand is 0.03 Å longer than the C–O bond of $CH_3C{\equiv}O^+SbF_6^-$[7] and 0.03 Å shorter than the C–O bonds of $CH_2{=}C{=}O$ (1.16 (1) Å)[12] and $(CH_3)HC{=}C{=}O$ (1.171 (2) Å).[13]

In the infrared spectrum of **2**, the 2092 cm^{-1} stretching frequency of the μ-CHCO ligand is 208 cm^{-1} lower in energy than the CO stretch of $CH_3C{\equiv}O^+$ (2300 cm^{-1}).[7] This indicates a reduced C–O bond order in **2** explainable in terms of ketene formulation **2k**. Indeed, the observed stretching frequency is similar to that observed for ketene (2151 cm^{-1})[8] and metal-substituted ketenes (1990–2018 cm^{-1}).[5d] The IR stretching frequency for the bridging carbonyl ligand of diiron complexes is sensitive to the positive charge delocalized in the $[C_5H_5(CO)Fe]_2(\mu\text{-CO})$ fragment. The IR stretching frequency for the bridging carbonyl ligand of **2** in CH_2Cl_2 (1847 cm^{-1}) is much higher than that of the μ-CH_2 compound $[C_5H_5(CO)Fe]_2(\mu\text{-CO})(\mu\text{-}CH_2)$ (**9**) (1780 cm^{-1})[10] and nearly as high as that of the cationic μ-CH compound **1** (1856 cm^{-1}).[2] This indicates extensive delocalization of positive charge into the iron framework of **2** and can be explained in terms of a significant contribution from ketene resonance structure **2k**.

The bridging carbon of the μ-CHCO ligand of **2** appears unusually far upfield in the ^{13}C NMR at δ 27.5. This contrasts with other diiron μ-alkylidene complexes, which generally show resonances between δ 135 and 200 for the μ-alkylidene carbon.[1,11] For example, the μ-CH_2 carbon of the cis Cp isomer of the bridging methylene complex **9** appears at δ 138.5.[10] While this comparatively large upfield shift of the bridging carbon in the μ-CHCO ligand of **2** is difficult to rationalize, we note that for free ketenes the terminal ($R_2C{=}$) carbon typically resonates at a similar high-field shift.[14] The one-bond ^{13}C–H coupling of 174 Hz for the μ-CHCO ligand is also indicative of considerable sp^2 character in the bridging carbon atom. The acylium carbon of the μ-CHCO ligand of **2** appears at δ 162.6 in the ^{13}C NMR, which is substantially upfield from the δ 197 shift of $CH_3C{\equiv}O^+SbF_6^-$.[15] This is consistent with enhanced electron donation to the acylium carbon of **2**.

The closest analogies to **2** are the complexes $C_5H_5(CO)_2Mn[\mu\text{-}C(CO)C_6H_5]Re(CO)_4$[16] and $C_5H_5(CO)_2Mn[\mu\text{-}C(CO)C_6H_4\text{-}p\text{-}CH_3]Mn(CO)_4$.[17] The formation of each of these compounds has been proposed to involve migration of coordinated CO to an alkylidyne ligand. Bridging ketene formulations were stressed by the authors in describing the structures of these complexes. In addition, Kreissl has discussed the structure of the mononuclear ketenyl complex $C_5H_5(CO)(MeC{\equiv}CNEt_2)WC(CO)C_6H_4CH_3$ in terms of resonance structures with single ($W{=}CR{-}C{\equiv}O$) and double ($W{-}CR{=}C{=}O$) bonds between the carbons of the ketenyl ligand.[18] These resonance structures are related to those we have used to describe **2**.

The geometry of the μ-$CHCNCMe_3$ ligand in complex **6** provides a direct experimental test of the bonding description used to explain the structural and spectral properties of the CO adduct **2**. As mentioned earlier, if the structure of **6** can be adequately described with only nitrilium formulation **6n**, then the C–N–C angle in **6** would be expected to be linear; however, if the ketenimine formulation **6k** is a significant resonance contributor, then the C–N–C unit of **6** should be nonlinear with the *tert*-butyl group laterally displaced parallel to the iron–iron axis. Indeed, the X-ray crystal structure shows that the C2–N–C3 angle of **6** is 169.5 (4)°. We consider this small deviation from linearity to be significant since the displacement of the *tert*-butyl group is parallel to the iron–iron axis as predicted by ketenimine formulation **6k**.

Overall the structural data obtained for **6** indicate that the bridging ketenimine formulation **6k** does make a contribution to the observed structure, although the degree of carbon–carbon double bond character in the μ-$CHCNCMe_3$ ligand of **6** appears to be less than in the corresponding C–C bond of the μ-CHCO ligand of **2**. This is reflected in the C–C bond length of the μ-$CHCNCMe_3$ ligand of **6** which, at 1.397 (5) Å, is 0.06 Å longer than that in the μ-CHCO ligand of **2** (1.338 (8) Å). In addition, the C≡N bond distance of 1.147 (4) Å in **6** falls in the range commonly observed for C≡N bonds.[19] The manifestation of this decreased p_y–p_y π overlap in **6** accords with the better electron donating ability of the nitrogen atom in the μ-$CHCNCMe_3$ ligand of **6** as compared to oxygen in the μ-CHCO ligand of **2**. The IR and $^{13}C\{^1H\}$ NMR spectra of **6** provide additional evidence for the importance of the contributing bridging ketenimine structure **6k**. The C≡N stretching frequency of the μ-$CHCNCMe_3$ ligand at 2232 cm^{-1} is below the range normally observed for organic nitrilium cations (2300–2370 cm^{-1}).[20] The μ-CO ligand of **6** shows a band at 1826 cm^{-1} which, like complex **2**, suggests partial delocalization of positive charge onto the diiron framework. Additionally, in the $^{13}C\{^1H\}$ NMR spectrum of **6** the resonance for the bridging carbon of the μ-$CHCNCMe_3$ ligand is observed at δ 61.6; this is a similar but smaller upfield shift compared with that seen for **2**.

Isocyanide addition to a mononuclear metal carbyne complex was previously observed by Fischer,[21] who reported that the alkylidyne complex $C_5H_5(CO)_2Mn{\equiv}CC_6H_5^+$ undergoes nucleophilic attack by $CNCMe_3$ to give the alkylidene complex $C_5H_5(CO)_2Mn{=}C(C_6H_5)CNC(CH_3)_3^+$.

Fenske–Hall Molecular Orbital Calculations. The experimental data outlined above all suggest that the carbon–carbon bonds in the μ-CHCO ligand of **2** and in the μ-CHCNR ligand of **6** possess some degree of p_y–p_y π character (taking the z axis to be the ligand axis), with a corresponding decrease in the bond order of the C–O bond. To gain further insight into the bonding in these systems, we have carried out Fenske–Hall molecular orbital calculations.[22] The geometry of the $[C_5H_5(CO)Fe]_2(\mu\text{-CO})$ fragment was based on the X-ray crystal structure of μ-CHCO complex **2**, idealized to C_s symmetry with local D_{5h} symmetry at the C_5H_5 rings. The geometry of this fragment was similar to the X-ray data for the

(12) Cox, A. P.; Thomas, L. F.; Sheridan, J. *Spectrochim. Acta* **1959**, *15*, 542–548.
(13) Bak, B.; Christiansen, J.; Kunstmann, K.; Nygaard, L.; Rastrup-Andersen, J. *J. Chem. Phys.* **1966**, *45*, 883–887.
(14) (a) Firl, J.; Runge, W. *Z. Naturforsch. B* **1974**, *29*, 393–398. (b) Runge, W. *Org. Magn. Reson.* **1980**, *14*, 25–31.
(15) The acylium carbon of $CH_3{}^{13}C{\equiv}O^+SbF_6^-$ in anhydrous HF appeared 30.9 ppm to lower field than $CF_3{}^{13}CO_2H$. Olah, G. A.; Tolgyesi, W. S.; Kuhn, S. J.; Moffatt, M. E.; Bastien, I. J.; Baker, E. B. *J. Am. Chem. Soc.* **1963**, *85*, 1328–1334.
(16) Orama, O.; Schubert, U.; Kreissl, F. R.; Fischer, E. O. *Z. Naturforsch. B* **1980**, *35B*, 82–85.
(17) Martin-Gil, J.; Howard, J. A. K.; Navarro, R.; Stone, F. G. A. *J. Chem. Soc., Chem. Commun.* **1979**, *1168*–1169.
(18) Kreissl, F. R.; Reber, G.; Müller, G. *Angew. Chem., Int. Ed. Engl.* **1986**, *25*, 643–644.
(19) See, for example: Karakida, K.; Fukuyama, T.; Kuchitsu, K. *Bull. Chem. Soc. Jpn.* **1974**, *47*, 299 and references therein.
(20) Olah, G. A.; Kiovsky, T. E. *J. Am. Chem. Soc.* **1968**, *90*, 4666–4672.
(21) (a) Fischer, E. O.; Schambeck, W.; Kreissl, F. R. *J. Organomet. Chem.* **1979**, *169*, C27–C30. (b) Fischer, E. O.; Schambeck, W. *J. Organomet. Chem.* **1980**, *201*, 311–318.
(22) Hall, M. B.; Fenske, R. F. *Inorg. Chem.* **1972**, *11*, 738–775.

Table III. Bond Lengths and Angles Used in Calculations

fragment	bond distances (in Å)		angles (in deg)	
$[C_5H_5(CO)Fe]_2(\mu\text{-}CO)$	Fe–Fe	2.550	Fe–(μ-C)–Fe	81.7
	Fe–(t-CO)	1.780	Fe–(μ-C)–O	139.1
	Fe–(μ-CO)	1.948	(μ-C)–Fe–(t-C)	89.2
	Fe–C_g[a]	1.730	Fe–Fe–C_g	137.6
	C–O(t-CO)	1.140	C_g–Fe–(t-C)	122.1
	C–O(μ-CO)	1.164	C_g–Fe–(μ-C)	118.3
	C–C	1.400		
	C–H	1.000		
μ-$CHCO^+$	Fe–C	1.994	Fe–(μ-C)–Fe	79.4
	C–C	1.340	Fe–(μ-C)–C	110.6
	C–O	1.135	H–(μ-C)–C	111.0
μ-$CHCNH^+$	Fe–C	1.980	Fe–(μ-C)–Fe	79.7
	C–C	1.397	Fe–(μ-C)–C	116.1
	C–N	1.147	H–(μ-C)–C	107.3
			C–N–H	169.5

[a] C_g is the center of gravity of the Cp group.

other calculated compounds and was kept constant. For calculations of both the acylium and nitrilium diiron compounds the μ-C–C–X angle was idealized at 180°. In the calculations of the bridging nitrilium complex, the bond lengths used for the μ-CHCNR ligand were taken from the X-ray structure of **6** and the *tert*-butyl group was replaced by a hydrogen atom at 1.00 Å. The key structural parameters used in the calculations are summarized in Table III. The local Cartesian coordinate system in the bridging ligand was selected such that the z axis of each atom was oriented along the carbon–carbon axis with the y axis parallel to the iron–iron axis, as illustrated below.

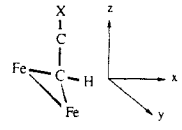

For comparison purposes, calculations of the acylium cation, CH_3CO^+, were performed with the same C–C and C–O bond lengths as found in the iron–acylium adduct. This simplifies interpretation of the overlap occupations by suppressing changes in the overlap due to changes in bond distances. Calculations were also performed on the adduct **2** and on the free acylium ion by using the reported bond distances for $CH_3CO^+SbF_6^-$[7] with very similar results.

It would have been convenient if the π character between the carbons of the bridging ligand in the adducts was manifested in a *single* occupied orbital having strong p_y character from these two carbons. However, due to the highly delocalized nature of the molecular orbitals, the calculation of $[C_5H_5(CO)Fe]_2(\mu\text{-}CO)(\mu\text{-}CHCO)^+$ showed no single MO having large C–C π_y character. Nevertheless, the net overlap populations between p_y orbitals on these two carbons summed over all occupied orbitals indicated significant π bonding between the two carbons. The overlap population of 0.225 for the carbon–carbon p_y overlap in the CO adduct **2** is much higher than that calculated for $CH_3C{\equiv}O^+$, 0.057. The higher p_y–p_y overlap population between the carbons of **2** compared with the carbons of $CH_3C{\equiv}O^+$ is accompanied by a lower p_y–p_y overlap population between carbon and oxygen in **2** compared with $CH_3C{\equiv}O^+$. These overlap populations are in agreement with bonding intermediate between acylium formulation **2a** and ketene formulation **2k**. Table IV summarizes the key net overlap populations.

Similarly, for the diiron isocyanide adduct, the p_y–p_y overlap population between the carbons of the μ-CHCNH ligand (0.179) is substantially larger than that seen for CH_3CNH^+ (0.032).

Bonding effects due to bending at nitrogen and displacement of the nitrogen substituent along a line parallel to the iron–iron axis were investigated with Fenske–Hall MO calculations.[23]

(23) In the series of calcuations, the Fe–μC distance was held at 1.98 Å to remove any ambiguity in the division of charge between iron and carbon.

Table IV. Selected Net Overlap Occupations

	bond lengths		net overlap populations			
	C–C	C–O	CCp_x	CCp_y	COp_x	COp_y
2	1.340	1.135[a]	0.112	0.225	0.403	0.352
	1.385	1.108	0.095	0.196	0.423	0.376
CH_3CO^+	1.340	1.135	0.058	0.058	0.441	0.441
	1.385	1.108[a]	0.047	0.047	0.459	0.459
CH_2CO	1.340	1.135	0.044	0.365	0.439	0.263
	1.385	1.108	0.036	0.338	0.456	0.285
	bond lengths		net overlap populations			
	C–C	C–N	CCp_x	CCp_y	CNp_x	CNp_y
6	1.397	1.147*	0.079	0.179	0.481	0.424
CH_3CNH^+	1.397	1.147	0.031	0.032	0.509	0.509
CH_2CNH	1.397	1.147	0.020	0.376	0.512	0.213

[a] C–C and C–X bond lengths for this compound taken from X-ray structure.

Table V. Torsion Angle Effects on Overlap Population of μ-C–C–NH

	CCp_x	CCp_y	CNp_x	CNp_y
	At ∠CNH = 169.5°			
90 (actual)	0.079	0.179	0.481	0.424
0	0.081	0.177	0.477	0.429
180	0.079	0.177	0.477	0.429
	At ∠CNH = 180°			
	0.079	0.177	0.481	0.426
	At ∠CNH = 120°			
90	0.073	0.227	0.491	0.310
0	0.114	0.173	0.364	0.438
180	0.107	0.171	0.361	0.439

Variations in overlap populations as a function of geometry are presented in Table V. Calculations on a linear nitrilium adduct (CNH angle = 180°) showed a small decrease in the p_y–p_y net overlap population. When the C–N–H angle was set at 169.5° and the hydrogen was rotated into the plane bisecting the iron–iron axis (H–CCN–H torsion angle = 0° or 180°), small decreases in the carbon–carbon p_y–p_y overlap population were observed. When the nonlinear nature of the μ-CHCNH ligand was magnified by setting the C–N–H angle at 120°, a great increase in the carbon–carbon p_y–p_y overlap population was noted and a dramatic dependence of that overlap population on the H–CCN–H torsion angle was seen.

These calculations support the notion that the nonlinearity of the μ-C—C≡N—CMe_3 ligand of **6** and the displacement of the *tert*-butyl group along a line parallel to the iron–iron axis are both significant.

Mulliken population analysis on the molecular orbital calculations indicated that the charges assigned to the entire $[C_5H_5(CO)Fe]_2(\mu\text{-}CO)$ fragment[23] of the μ-CHCO cation (+1.084) and of the μ-CHCNH cation (+0.920) were similar to that calculated for the μ-CH cation (+1.259) and were much greater than that calculated for the neutral μ-CH_2 complex (+0.432). This greater positive charge on the diiron fragment helps to explain the high-frequency μ-CO band seen for the μ-CHCO, μ-$CHCNCMe_3$, and μ-CH cations relative to the neutral μ-CH_2 complex.

Experimental Section

General. ^1H NMR spectra were normally obtained on a Bruker WP270 spectrometer or where indicated on a Bruker WP200 spectrometer. ^{13}C NMR spectra were normally obtained on a JEOL FX200 spectrometer (50.1 MHz) or where indicated on a Bruker AM500 spectrometer (125.76 MHz). $Cr(acac)_3$ (0.07 M) was added to ^{13}C NMR samples as a shiftless relaxation agent. Infrared spectra were measured on a Beckman 4230 or Mattson Polaris (FT) spectrometer. Mass spectra were determined on a Kratos MS-80. Elemental analyses were performed by Galbraith Laboratories, Inc. (Knoxville, TN) or by Schwarzkopf Laboratories (Woodside, NY).

Air-sensitive materials were manipulated in an inert atmosphere glovebox or by standard high-vacuum and Schlenk techniques. Diethyl

ether, THF, hexane, and C_6D_6 were distilled immediately prior to use from purple solutions of sodium and benzophenone. CH_2Cl_2 and CD_2Cl_2 were dried over CaH_2. CD_3CN and $(CD_3)_2CO$ were dried over CaH_2 and B_2O_3, respectively.

Computational Details. Molecular orbital calculations were performed on a DEC VAX-8600 computer system with use of the Fenske–Hall molecular orbital method.[22] Clementi's free atom double-ζ Hartree–Fock functions[24] were used for C, N, and O. All except valence shell p functions were curve fit to single-ζ form by using the criterion of maximum overlap.[25] A value of 1.16 was used for the hydrogen 1s atomic orbital. The functions 1s–3d for iron were taken from the tables of Richardson, Nieuwport, Powell, and Edgell.[26] The exponents for the single-ζ 4s and 4p orbitals were set to 2.0.

$[C_5H_5(CO)Fe]_2(\mu\text{-}CO)(\mu\text{-}CHCO)^+PF_6^-$ (2). A slurry of **1** (204 mg, 0.42 mmol) in CH_2Cl_2 (8 mL) was stirred under an atmosphere of carbon monoxide (600 Torr, 300 mL, 9.7 mmol) for 1 h at 0 °C. The reaction mixture was then warmed to ambient temperature and stirred for an additional 90 min. The volume of solvent was reduced under vacuum (to 5 mL) and diethyl ether (5 mL) was added. The resulting dark-purple precipitate was isolated by filtration, washed with ether (3 × 5 mL), and dried under vacuum to give **2** (194 mg, 90%). ^1H NMR (acetone-d_6, 200 MHz) δ 6.94 (s, μ-CH), 5.67 (s, 10 H, C_5H_5); ^{13}C NMR (acetone-d_6, 0 °C) δ 249.6 (μ-CO), 209.2 (CO), 162.6 (μ-CHCO), 91.1 (d, $J_{^{13}CH}$ = 183 Hz, C_5H_5), 27.5 (d, $J_{^{13}C-H}$ = 174 Hz in CD_3NO_2, μ-CHCO); IR (KBr) 2092 (s), 2002 (s), 1819 (s) cm^{-1}; IR (CH_2Cl_2) 2092 (s), 2012 (s), 1847 (s) cm^{-1}. Anal. Calcd for $C_{15}H_{11}PF_6Fe_2O_4$: C, 35.20; H, 2.17; P, 6.05. Found: C, 35.13; H, 2.34; P, 6.07.

$[C_5H_5(CO)Fe]_2(\mu\text{-}CO)(\mu\text{-}CH^{13}CO)^+PF_6^-$ (2-^{13}C). Reaction of **1** (133 mg, 0.28 mmol) with ^{13}CO (90% enriched) as described for **2** led to the isolation of **2**-^{13}C (116 mg, 82%). ^1H NMR (acetone-d_6, 200 MHz) δ 6.94 (d, $J_{^{13}C-H}$ = 4.4 Hz, $CH^{13}CO$), 5.67 (s, 10 H, C_5H_5); IR (KBr) 2057 (s), 2002 (s), 1820 (s) cm^{-1}.

$[C_5H_5(CO)Fe]_2(\mu\text{-}CO)(\mu\text{-}CHCHO)$ (3). THF (8 mL) was condensed onto a solid mixture of **2** (160 mg, 0.31 mmol) and $Et_4N^+HFe(CO)_4^-$ (145 mg, 0.48 mmol) at −78 °C. A deep red solution rapidly formed. After the solution was stirred at −78 °C for 90 min, the solvent was evaporated under vacuum at room temperature. The residue was extracted into CH_2Cl_2 (5 mL) and chromatographed on an alumina column. Elution with 1:1 hexane:diethyl ether afforded a small quantity of $[C_5H_5(CO)Fe]_2(\mu\text{-}CO)(\mu\text{-}CH_2)$. Elution with 1:1 acetone:diethyl ether then afforded a purple-red band, which was a mixture of **3** and $Et_4N^+PF_6^-$. The organometallic component was extracted into ether (~100 mL) and filtered through a plug of Celite. Evaporation of solvent under vacuum, followed by washing with hexane (5 mL) and drying, afforded **3** as a deep red crystalline solid (80 mg, 70%). ^1H NMR (C_6D_6, 200 MHz) δ 10.26 (d, J = 9.3 Hz, CH), 9.63 (d, J = 9.3 Hz, CH), 4.07 (s, 10 H, C_5H_5); $^{13}C\{^1H\}$ NMR (C_6D_6) δ 265.0 (μ-CO), 212.4 (CO), 202.2 (CHO), 156.1 (μ-CH), 87.7 (C_5H_5); IR (Nujol) 1990 (s), 1956 (m), 1800 (s), 1615 (m) cm^{-1}. Anal. Calcd for $C_{15}H_{12}Fe_2O_4$: C, 48.96; H, 3.29; Fe, 30.36. Found: C, 49.21; H, 3.44; Fe, 30.09.

$[C_5H_5(CO)Fe]_2(\mu\text{-}CO)(\mu\text{-}CHCO_2H)$ (4). H_2O (3 mL) was added via syringe to a vigorously stirred slurry of **2** (134 mg, 0.26 mmol) in CH_2Cl_2 (10 mL) at room temperature. A red precipitate formed immediately. The solid was isolated by filtration, washed with H_2O (5 mL), and dried under vacuum. Recrystallization from THF/hexane afforded **4** as a red crystalline solid (50 mg, 50%). ^1H NMR (acetone-d_6, 200 MHz) δ 10.34 (s, μ-CH), 9.85 (br s, CO_2H), 4.84 (s, 10 H, C_5H_5); ^{13}C NMR (acetone-d_6) 269.6 (μ-CO), 211.8 (CO), 184.3 (CO_2H), 142.3 ($J_{^{13}C-H}$ = 139 Hz, μ-CH), 87.5 ($J_{^{13}C-H}$ = 178 Hz, C_5H_5); IR (KBr) 2930 (m, br), 1988 (s), 1957 (m), 1788 (s), 1630 (m), 1440 (w), 1284 (m), 1168 (m) cm^{-1}. Anal. Calcd for $C_{15}H_{12}Fe_2O_5$: C, 46.92; H, 3.15; Fe, 29.09. Found: C, 46.78; H, 3.44; Fe, 28.91.

$[C_5H_5(CO)Fe]_2(\mu\text{-}CO)(\mu\text{-}CHCONH_2)$ (5). A slurry of **2** (209 mg, 0.41 mmol) in CH_2Cl_2 (15 mL) was placed under an atmosphere of anhydrous ammonia at room temperature. A red solution rapidly formed. NH_3 and CH_2Cl_2 were evaporated under vacuum and THF (10 mL) was added. The red solid present was isolated by filtration, washed with THF (3 × 2.5 mL) to remove $NH_4^+PF_6^-$, and dried under vacuum to give **5** (43 mg, 28%). ^1H NMR (DMSO-d_6, 200 MHz) δ 10.74 (s, μ-CH), 7.25 (br s, NH), 6.29 (br s, NH), 4.90 (s, 10 H, C_5H_5); ^{13}C NMR (DMSO-d_6) δ 271.7 (μ-CO), 211.9 (CO), 183.4 ($CONH_2$), 153.3 ($J_{^{13}C-H}$ = 138 Hz, μ-CH), 84.1 ($J_{^{13}C-H}$ = 178 Hz, C_5H_5); IR (Nujol) 3515 (m), 3384 (m), 1982 (s), 1937 (m), 1755 (s), 1629 (m), 1579 (m), 1338 (m), 1212 (m), 1131 (m) cm^{-1}. Anal. Calcd for $C_{15}H_{13}NFe_2O_4$: C, 47.04; H, 3.42; N, 3.66. Found: C, 47.52; H, 3.30; N, 3.51.

$[C_5H_5(CO)Fe]_2(\mu\text{-}CO)[\mu\text{-}CHCNC(CH_3)_3]^+PF_6^-$ (6). *tert*-Butyl isocyanide (0.04 mL, 0.35 mmol) was added by syringe to a slurry of **1** (150 mg, 0.31 mmol) in CH_2Cl_2 (10 mL) cooled to −78 °C. Volatile material was evaporated under vacuum at room temperature. The residue was dissolved in the minimum of CH_2Cl_2 and filtered. Diethyl ether (10 mL) was added to afford a deep purple-red precipitate which was isolated by filtration, washed with diethyl ether (3 × 5 mL), and dried under vacuum to give **6** (110 mg, 63%). ^1H NMR (CD_2Cl_2, 200 MHz) δ 7.73 (s, μ-CH), 5.14 (s, 10 H, C_5H_5), 1.51 (s, $C(CH_3)_3$); $^{13}C\{^1H\}$ NMR (CD_2Cl_2, 125.76 MHz) δ 256.6 (μ-CO), 209.6 (CO), 125.8 (*C*NCMe$_3$), 89.0 (C_5H_5), 62.4 (*C*(CH$_3$)$_3$), 61.6 (μ-CHR), 29.4 (CH_3); IR (CH_2Cl_2) 2232 (m), 2000 (s), 1975 (w), 1826 (m) cm^{-1}. Anal. Calcd for $C_{19}H_{20}NF_6Fe_2O_3P$: C, 40.25; H, 3.56; N, 2.47. Found: C, 40.23; H, 3.61; N, 2.48.

$[C_5H_5(CO)Fe]_2(\mu\text{-}CO)[\mu\text{-}C(CH_3)CNC(CH_3)_3]^+BF_4^-$ (8). Reaction of **7** (604 mg, 1.37 mmol) with *tert*-butyl isocyanide (0.20 mL, 1.77 mmol) followed by workup as described for **6** gave **8** (640 mg, 89%, 4.1:1.2:1.0 mixture of cis:cis′:trans Cp isomers). ^1H NMR (CD_2Cl_2), major cis isomer, δ 5.14 (s, 10 H, C_5H_5), 2.90 (s, CH_3), 1.50 (s, $C(CH_3)_3$); minor cis isomer, δ 5.04 (s, $C(CH_3)_3$); minor cis isomer, δ 5.04 (s, 10 H, C_5H_5), 2.44 (s, CH_3), 1.81 (s, $C(CH_3)_3$); trans isomer, δ 5.11 (s, 5 H, C_5H_5), 4.99 (s, 5 H, C_5H_5), 2.70 (s, CH_3), 1.65 (s, $C(CH_3)_3$); $^{13}C\{^1H\}$ NMR (CD_2Cl_2, 125.76 MHz), major cis isomer, δ 256.9 (μ-CO), 209.9 (CO), 125.4 (*C*NCMe$_3$), 90.7 (C_5H_5), 88.9 (μ-*C*(CH$_3$)R), 61.5 (*C*(CH$_3$)$_3$), 37.3 (μ-C(*C*H$_3$)R), 29.4 (C(*C*H$_3$)$_3$); minor cis isomer, δ 257.3 (μ-CO), 208.8 (CO), 127.0 (*C*NCMe$_3$), 90.0 (C_5H_5), 82.6 (*C*(CH$_3$)R), 62.6 (*C*(CH$_3$)$_3$), 37.5 (μ-C(*C*H$_3$)R), 30.5 (C(*C*H$_3$)$_3$); trans isomer, δ 207.9 (CO), 91.6 (C_5H_5), 91.2 (C_5H_5), 87.1 (μ-*C*(CH$_3$)R), 62.3 (*C*(CH$_3$)$_3$), 29.6 (C(*C*H$_3$)$_3$), μ-CO, *C*NCMe$_3$, and μ-C(*C*H$_3$)R not observed; IR (CH_2Cl_2) 2220 (m), 2000 (s), 1980 (m), 1822 (m) cm^{-1}. Anal. Calcd for $C_{20}H_{22}NBF_4Fe_2O_3$: C, 45.94; H, 4.24; N, 2.68. Found: C, 45.83; H, 4.56; N, 2.77.

X-ray Crystal Structure Determination of 6. Crystals of **6** suitable for X-ray diffraction study were obtained by vapor diffusion between a dichloromethane solution of **6** and diethyl ether. A single crystal of approximate dimensions 0.40 × 0.38 × 0.20 mm was mounted in air for the X-ray study. Preliminary examination of the crystal on a Syntex-Nicolet-P1 diffractometer showed the crystal to be monoclinic. The

Table VI. Summary of Crystal Data and Intensity Collection[a] for **6**

empirical formula	$C_{19}H_{20}BF_4Fe_2NO_3$
formula wt	508.870
cryst dimens, mm	0.40 × 0.38 × 0.20
temp, K	113
cell parameters	
a, Å	10.771 (2)
b, Å	11.420 (2)
c, Å	18.092 (3)
β	106.09 (1)
space group	$P2_1/c$
Z	4
density, calcd, g/cm^3	1.76
absorption coeff, μ, cm^{-1}	15.02
Nicolet diffractometer[b]	$P\bar{1}$
scan type	θ–2θ
scan range	
deg below 2θ Kα_1	0.9
deg above 2θ Kα_2	0.9
scan speed, deg/min	2.93–29.3
background/scan ratio	0.33
2θ limits, deg	3.5–50.7
max sin θ/λ, Å^{-1}	0.65
unique data	
theoretical	4781
$F_o > 3\sigma(F_o)$	3964
P; weight = $[\sigma^2(F) + p^2F^2]^{-1}$	0.0016
discrepancy indices	
R_1 (obsd data)	5.13
R_2 (obsd data)	4.89
goodness of fit	1.403
observation/variable ratio	13.5
final difference ρ_{max}, e/Å^3	0.54

[a] Method similar to: Haller, K. J.; Enemark, J. H. *Inorg. Chem.* **1978**, *17*, 3552. Scattering factor tables from *International Tables for X-ray Crystallography*; Kynoch Press: Birmingham, England, 1974; Vol. IV. [b] Diffractometer equipped with a graphite monochromated molybdenum Kα radiation source.

(24) Clementi, E.; Raimondi, D. L. *J. Chem. Phys.* **1963**, *38*, 2686–2689.
(25) Radtke, D. D. Ph.D. Dissertation, University of Wisconsin, Madison, WI, 1966.
(26) Ricardson, J. W.; Nieuwport, W. C.; Powell, R. R.; Edgell, W. F. *J. Chem. Phys.* **1962**, *36*, 1057–1061.

observed systematic absences of $h0l$ ($l = 2n+1$) and $0k0$ ($k = 2n + 1$) uniquely define the space group as $P2_1/c$. The unit cell and data collection parameters are summarized in Table VI. Throughout data collection four standard reflections from diverse regions of reciprocal space were measured every 50 reflections. The intensities of the standard reflections showed no systematic variations during data collection.

Data reduction, solution, and refinement of the structure were performed with the SHELXTL structure determination package (Nicolet XRD Corp., Madison, WI). Direct methods were used to locate the positions of the iron atoms. Subsequent difference Fourier maps revealed the location of the remaining non-hydrogen atoms. All hydrogen atoms were included as fixed contributions at idealized locations except the carbene hydrogen H(1) which was located and isotropically refined. Psi scan absorption corrections were found not to lead to any improvement in the refinement and were consequently omitted.

Some disorder in the PF_6 counterion was evident, particularly from the large thermal elipsoids of the fluorine atoms. However, difference Fourier maps failed to suggest a suitable disorder model. The final refinement converged at $R = 0.051$ and $R_w = 0.049$. The magnitude of the largest peak on the final electron density difference map was 0.54 e/Å^3.

Acknowledgment. Support from the National Science Foundation is gratefully acknowledged. We thank Professor Richard F. Fenske, Paul T. Czech, and Dr. Kenneth J. Haller for helpful discussions. M.C. thanks the Science and Engineering Research Council (U.K.) for a NATO postdoctoral fellowship. G.P.N. thanks the Wisconsin Alumni Research Foundation for a fellowship. M.S.K. thanks SOHIO for a fellowship.

Supplementary Material Available: Tables of atomic coordinates, bond distances, bond angles, and anisotropic thermal parameters (6 pages); listing of structure factors (calculated vs observed) (28 pages). Ordering information is given on any current masthead page.

IR Flash Kinetic Spectroscopy of Transients Generated by Irradiation of $(\eta^5\text{-}C_5H_5)Co(CO)_2$ in the Gas Phase and in Solution

Eric P. Wasserman, Robert G. Bergman,* and C. Bradley Moore*

Contribution from the Department of Chemistry, University of California, and the Materials and Chemical Sciences Division of the Lawrence Berkeley Laboratory, Berkeley, California 94720.
Received February 5, 1988. Revised Manuscript Received April 11, 1988

Abstract: The photoinduced ligand substitution chemistry of $(\eta^5\text{-}C_5H_5)Co(CO)_2$ in the gas and solution phases has been studied by using laser flash kinetic spectroscopy with fast IR detection. The data are consistent with primary loss of one CO to form an unsaturated species which then reacts with ligands such as C_2H_4 in the gas phase or with $P(n\text{-}C_4H_9)_3$ in cyclohexane solution. The rates of bimolecular ligand addition reactions have been measured for several ligands. In general, the unsaturated intermediate reacts with ligands at rates close to those of diffusion in both media, which indicates that the open site of the coordination sphere may be only weakly solvated in alkane solutions. Solvation complexes of this intermediate with benzene and tetrahydrofuran in cyclohexane solution were produced; these solvates are far less reactive than the cyclohexane solvate. The benzene solvate appears to react with ligand through both direct and indirect pathways. The rate constants for these reactions have been determined.

The role played by solvent molecules in organometallic reactions is not well-understood. This is especially true for nonaqueous solutions, whose physical properties have received relatively little attention, given the enormous experimental literature on the effect of solvent on the reactivity and thermodynamics of organic molecules and of simple inorganic ions.[1] It is known, however, that varying the solvent has a profound effect on the reactivity of coordinatively unsaturated organometallic species.[2] Coordination of solvent has a profound effect on the rate of carbonyl migratory insertion,[3a] one of the most well-studied organometallic transformations.[3b,c] In the case of octahedral WL_6 complexes,[3d] the presence of a solvent molecule effectively locks the pentacoordinate WL_5 photoproduct into distinguishable octahedral geometries, an interaction so strong as to lead Dobson et al. to coin the term "token ligand" for the occupant solvent molecule. The recent discovery of solvates of C–H activating fragments in ultracold matrices[4] has raised our curiosity about their role in solution-phase mechanisms, since the solvating hosts range from noble gas to potentially reactive matrices.

Within the past several years, the technique of flash photolysis, combined with fast detection of transient species, has led to significant contributions to the understanding of fundamental problems in organometallic chemistry.[5] In this work, an important unsaturated organometallic fragment, $CpCo(CO)$ ($Cp = \eta^5\text{-}C_5H_5$), is studied in both the gas and solution phases. The extent to which solvent occupation and stabilization of the open site affects its reactivity is determined for two-electron donor ligands.

$CpCo(CO)_2$ was settled on as a good starting point for our study for several reasons. A volatile (partial pressure at 300 K $\simeq$ 1.1 Torr), light-sensitive compound, it lends itself to gas- as well as liquid-phase photochemical study. Not only is it a congener of the second- and third-row C–H activating compounds $Cp^{(*)}M(CO)_2$ (M = Rh, Ir; $Cp^* = \eta^5\text{-}C_5Me_5$)[6] but $CpCo(CO)_2$ is also

(1) Some research on physical properties of nonelectrolytic solutions has been collected in *Physical Chemistry of Organic Solvent Systems*; Covington, A. K., Dickinson, T., Eds.; London: Plenum Press, 1973.

(2) See, for example: (a) Belt, S. T.; Haddleston, D. M.; Perutz, R. N.; Smith, B. P. H.; Dixon, A. J. *J. Chem. Soc., Chem. Commun.* **1987**, 1347. (b) Church, S. P.; Grevels, F.-W.; Hermann, H.; Schaffner, K. *Inorg. Chem.* **1985**, *24*, 418. (c) Church, S. P.; Grevels, F.-W.; Herrmann, H.; Kelly, J. M.; Klotzbuecher, W. E.; Schaffner, K. *J. Chem. Soc., Chem. Commun.* **1985**, 594. (d) Giordano, P. J.; Wrighton, M. S. *Inorg. Chem.* **1977**, *16*, 166.

(3) (a) Wax, M. J.; Bergman, R. G. *J. Am. Chem. Soc.* **1981**, *103*, 7028. (b) Kuhlman, E. J.; Alexander, J. J. *Coord. Chem. Rev.* **1980**, *33*, 195–225. (c) Alexander, J. J. *The Chemistry of the Metal–Carbon Bond*; Hartley, F. R., Ed.; Wiley: New York, 1985; Vol. 2, Chapter 5. (d) Dobson, G. R.; Hodges, P. M.; Healy, M. A.; Poliakoff, M.; Turner, J. J.; Firth, S.; Asali, K. J. *J. Am. Chem. Soc.* **1987**, *109*, 4218.

(4) Rest, A. J.; Whitewell, I.; Graham, W. A. G.; Hoyano, J. K.; McMaster, A. D. *J. Chem. Soc., Dalton Trans.* **1987**, 1181.

(5) For an excellent review on the progress in this area, cf.: Poliakoff, M.; Weitz, E. *Advances in Organometallic Chemistry*; Stone, F. G. A., Ed.; Academic Press: New York, 1986; Vol. 25, p 277.

(6) Hoyano, J. K.; Graham, W. A. G. *J. Am. Chem. Soc.* **1982**, *104*, 3723.

0002-7863/88/1510-6076$01.50/0